SOFTENING AND SNAP-THROUGH BEHAVIOR OF REINFORCED ELEMENTS

By C. Bosco[1] and A. Carpinteri,[2] Member, ASCE

ABSTRACT: The writers present a fracture mechanics model for reinforced concrete collapse, which is a refinement of that proposed previously, based on compliance and stress-intensification concepts. In this case, a crack-opening displacement congruence condition replaces the rotational congruence condition, while the reinforcement reactions are applied directly to the crack surfaces and not as closing forces at infinity. The theoretical results confirm a transition from ductile to brittle collapse by varying a nondimensional brittleness number defined in previous contributions. In addition, with the present model, yielding or slippage of reinforcement can precede or follow crack propagation in concrete. The moment-versus-rotation response presents softening and snap-through behaviors and is substantially in agreement with the experimental results. Such a theoretical approach appears to be very useful in estimating the minimum reinforcement for members in flexure.

INTRODUCTION

The application of fracture mechanics to reinforced concrete elements and, more generally, to fiber-reinforced materials, shows different failure modes in connection with different size scales. Recently, it has been proven experimentally that even the minimum content of reinforcement, which enables the element to prevent brittle failure, depends on the size scale (Bosco et al. 1990a). With a classical approach these results cannot be found and they are not predictable.

The compliance approach, proposed previously (Okamura et al. 1973, 1975; Carpinteri 1984), allows the calculation of the deformations (rotation and/or elongation) in a cracked element (without reinforcement) under bending moment and/or axial force. When a cracked reinforced element is considered, the same concepts can be applied, and the statically undetermined reaction of reinforcement is obtained, imposing a local congruence condition at the cracked section.

While the transition from brittle to ductile failure of the cracked reinforced element is not significantly influenced by the assumption of a rotational or a displacement congruence condition of the cracked section, some other aspects, such as the deformation of the element, seem more affected.

In fact, when a rotational congruence condition is imposed, the model does not predict local rotation due to the presence of the cracked section until yielding of reinforcement is reached (Carpinteri 1984). However, though the actual phenomenon is, in effect, more complex due to debonding and slippage of reinforcement from tests carried out on initially uncracked elements with low reinforcement (Bosco et al. 1990b), generally, it appears

[1]Assoc. Prof., Dept. of Struct. Engrg., Politecnico di Torino, 24 Corso Duca degli Abruzzi, 10129 Torino, Italy.

[2]Prof., Dept. of Struct. Engrg., Politecnico di Torino, 24 Corso Duca degli Abruzzi, 10129 Torino, Italy.

Note. Discussion open until January 1, 1993. To extend the closing date one month, a written request must be filed with the ASCE Manager of Journals. The manuscript for this paper was submitted for review and possible publication on February 12, 1991. This paper is part of the ***Journal of Engineering Mechanics***, Vol. 118, No. 8, August, 1992. ©ASCE, ISSN 0733-9399/92/0008-1564/$1.00 + $.15 per page. Paper No. 1386.

that, after the first cracking, crack propagation occurs before the yielding limit of reinforcement is reached.

The last aspects seem to have small importance compared with those concerning the failure characteristics (ductile or brittle), but the determination of more accurate relations representing the actual structural response is not of negligible interest.

In this paper, the writers apply a compliance model of fracture mechanics to a cracked element using a crack-opening displacement congruence condition that allows good agreement with the experimental results, without losing any other positive characteristic already obtained by similar methods.

Displacement Congruence Condition and Statically Undetermined Reaction of Reinforcement

The relationship between load and deformation of a cracked member that undergoes multiple loads simultaneously and behaves elastically is obtained by a superimposed effect on the deformation (Okamura et al. 1973, 1975; Carpinteri 1981, 1984).

Let us consider the cracked member shown in Fig. 1, simultaneously subjected to bending moment M and closing forces P applied on the crack surfaces. The evaluation of the crack opening displacement $\Delta\delta_{PM}$, produced by the moment M, together with the crack opening displacement $\Delta\delta_{PP}$, produced by the forces P, both measured at the points where the forces P are applied, provides, by linear superposition, the total displacement

$$\Delta\delta = \Delta\delta_{PM} + \Delta\delta_{PP} = \lambda_{PM}M - \lambda_{PP}P \quad \ldots\ldots\ldots\ldots\ldots\ldots\ldots\ldots (1)$$

where λ_{PM} and λ_{PP} = the compliances of the element, due to the crack's existence.

The factors λ_{PM} and λ_{PP} can be derived from energy methods, considering the moment M acting simultaneously with the forces P.

If G and E are, respectively, the strain energy release rate and the Young's modulus of the material (the Poisson ratio ν is considered negligible), it follows that the variation ΔW of the total potential energy is given by

$$\Delta W = \int_0^c G_M b\,dx + \int_c^a G_{(M+P)} b\,dx = \int_0^c \frac{K_{IM}^2}{E} b\,dx$$

$$+ \int_c^a \frac{(K_{IM} + K_{IP})^2}{E} b\,dx = \int_0^c \frac{K_{IM}^2}{E} b\,dx + \int_c^a \frac{K_{IM}^2}{E} b\,dx$$

$$+ \int_c^a \frac{K_{IP}^2}{E} b\,dx + 2\int_c^a \frac{K_{IM}K_{IP}}{E} b\,dx = \int_0^a \frac{K_{IM}^2}{E} b\,dx$$

$$+ \int_c^a \frac{K_{IP}^2}{E} b\,dx + 2\int_c^a \frac{K_{IM}K_{IP}}{E} b\,dx \quad \ldots\ldots\ldots\ldots\ldots\ldots\ldots\ldots (2)$$

where K_{IM} and K_{IP} = the stress-intensity factors due to bending moment M and forces P, respectively.

Using Clapeyron's theorem, we also have

$$\Delta W = \frac{1}{2} M\Delta\varphi_{MM} + \frac{1}{2} P\Delta\delta_{PP} + \frac{1}{2}(P\Delta\delta_{PM} + M\Delta\varphi_{MP}) \quad \ldots\ldots\ldots\ldots (3)$$

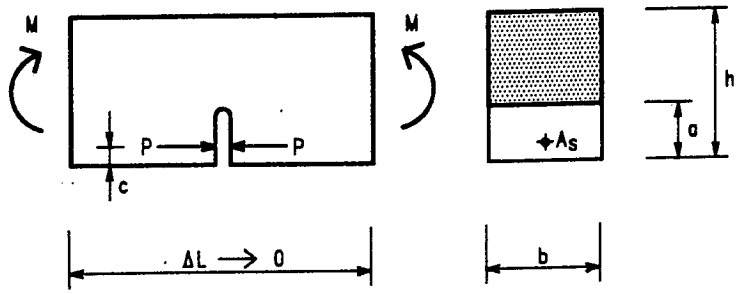

FIG. 1. Cracked Element

Recalling that Betti's theorem provides $P\Delta\delta_{PM} = M\Delta\varphi_{MP}$, from (2) and (3) it descends

$$\frac{1}{2} P\Delta\delta_{PP} = \int_c^a \frac{K_{IP}^2}{E} b\, dx \quad \ldots\ldots (4a)$$

$$P\Delta\delta_{PM} = 2\int_c^a \frac{K_{IM}K_{IP}}{E} b\, dx \quad \ldots\ldots (4b)$$

However, the stress-intensity factor produced at the crack tip by moment M can be expressed as (Okamura et al. 1973, 1975)

$$K_{IM} = \frac{M}{h^{3/2}b} Y_M(\xi) \quad \ldots\ldots (5a)$$

while the stress-intensity factor produced by the eccentric forces P acting at the level of reinforcement, i.e., at a distance c from the lower edge of the beam, is equal to

$$K_{IP} = \frac{P}{h^{1/2}b} Y_P\left(\frac{c}{h}, \xi\right) \quad \ldots\ldots (5b)$$

where

$$Y_P\left(\frac{c}{h}, \xi\right) = F\left(\frac{c}{a}, \xi\right) \frac{2}{\sqrt{\pi\xi}} \quad \ldots\ldots (6)$$

Function $Y_M(\xi)$ in (5a) for $\xi = a/h \leq 0.7$, is given by (Tada et al. 1963)

$$Y_M(\xi) = 6\,(1.99\xi^{1/2} - 2.47\xi^{3/2} + 12.97\xi^{5/2} - 23.17\xi^{7/2} + 24.80\xi^{9/2}) \quad .. (7)$$

while function $F(c/a, \xi)$ in (6) is expressed as

$$F\left(\frac{c}{a}, \xi\right) = \frac{3.52\left(1 - \frac{c}{a}\right)}{\left(1 - \frac{a}{h}\right)^{3/2}} - \frac{4.35 - 5.28\frac{c}{a}}{\left(1 - \frac{a}{h}\right)^{3/2}}$$

$$+ \left\{\frac{1.30 - 0.30\left(\frac{c}{a}\right)^{3/2}}{\left[1 - \left(\frac{c}{a}\right)^2\right]^{1/2}} + 0.83 - 1.76\frac{c}{a}\right\}\left[1 - \left(1 - \frac{c}{a}\right)\frac{a}{h}\right] \quad \ldots\ldots (8)$$

for $a/h < 1$, $c/a < 1$.

Substituting (5*b*) into (4*a*) and dividing by P^2, the compliance λ_{PP} (displacement produced by $P = 1$), can be expressed as

$$\lambda_{PP} = \frac{2}{bE} \int_{c/h}^{\xi} Y_P^2 \left(\frac{c}{h}, \xi\right) d\xi \quad (9)$$

while substituting (5*a*) and (5*b*) in (4*b*) and dividing by the product PM, the compliance λ_{PM} (displacement produced by $M = 1$), can be expressed in the form

$$\lambda_{PM} = \lambda_{MP} = \frac{2}{hbE} \int_{c/h}^{\xi} Y_P \left(\frac{c}{h}, \xi\right) Y_M(\xi)\, d\xi \quad (10)$$

Function $Y_P(c/h, \xi)$ is plotted in Fig. 2, for $c/h = 0.05, 0.10, 0.15$, together with function $Y_M(\xi)$. For each value of the ratio c/h, it is possible to observe that function Y_P tends to infinity for $\xi \rightarrow c/h^+$ and $\xi \rightarrow 1^-$. As a consequence, the stress-intensity factor K_{IP}, given by (5*b*), presents a minimum for an intermediate value of the crack depth ξ between c/h and 1.

Now let the forces P transmitted by reinforcement to the adjacent matrix surfaces be equal to

$$P = \sigma_s A_s \quad (11)$$

where A_s = the area of reinforcement; and σ_s = the related stress.

If the displacement discontinuity in the cracked cross section at the level of reinforcement is assumed to be zero up to the moment of yielding or slippage of the reinforcement

$$\Delta\delta = \Delta\delta_{PM} + \Delta\delta_{PP} = 0 \quad (12)$$

we obtain the displacement congruence condition that allows us to obtain the unknown force P as a function of the applied moment M. In fact, from (9), (10), and (12), and considering (1), it follows

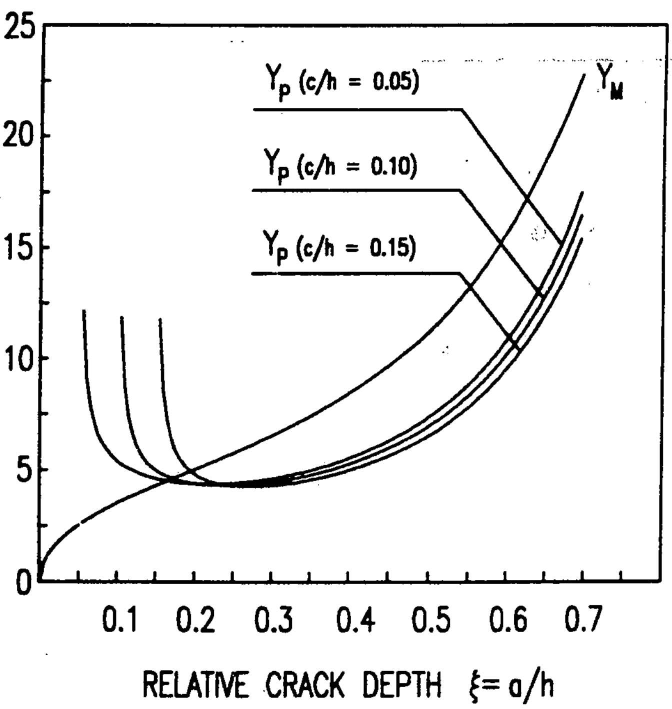

FIG. 2. Shape Functions Depending on Relative Crack Depth

$$\frac{Ph}{M} = \frac{1}{r''\left(\frac{c}{h}, \xi\right)} \qquad (13)$$

where

$$r''\left(\frac{c}{h}, \xi\right) = \frac{\int_{c/h}^{\xi} Y_P^2(\xi)\, d\xi}{\int_{c/h}^{\xi} Y_M(\xi) Y_P\left(\frac{c}{h}, \xi\right) d\xi} = \frac{\lambda_{PP}}{\lambda_{PM} h} \qquad (14)$$

Considering a rigid, perfectly plastic behavior of the reinforcement, the moment of plastic flow or slippage is obtained from (13)

$$M_P = P_P h r''\left(\frac{c}{h}, \xi\right) \qquad (15)$$

where $P_P = f_y A_s$ = the yielding (or pulling-out) force, achieved when $\sigma_s = f_y$ (yielding stress of reinforcement).

The statically undetermined reaction of the reinforcement is represented in Fig. 3, against the relative crack depth, for $c/h = 0.05, 0.10, 0.15$. The force transmitted by the reinforcement is always increasing in the whole range of validity of function $Y_M(\xi)$, i.e., for $c/h \leq \xi \leq 0.7$.

Combined Stress-Intensity Factor

By superposition, the stress intensity factor at the crack tip is [see (5*a*) and (5*b*)]

$$K_I = \frac{M}{h^{3/2} b} Y_M(\xi) - \frac{P}{h^{1/2} b} Y_P\left(\frac{c}{h}, \xi\right) \qquad (16)$$

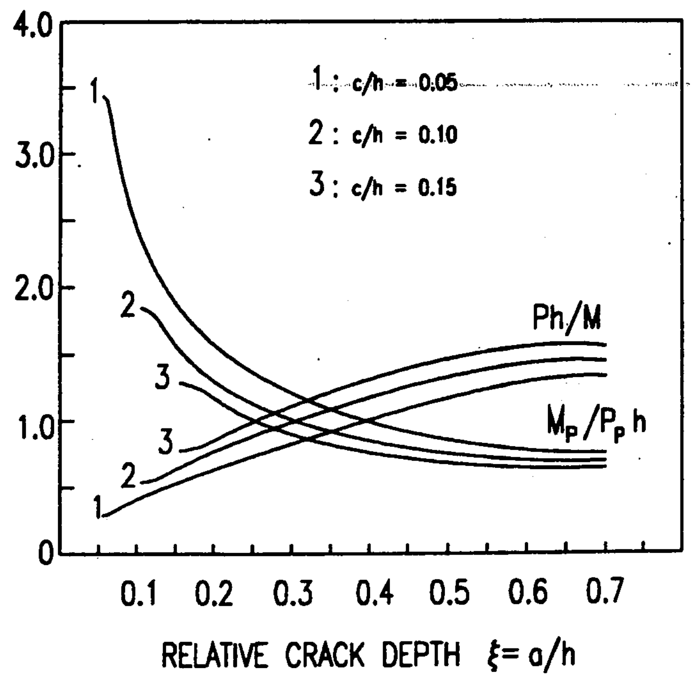

FIG. 3. Statically Undetermined Reaction of Reinforcement versus Relative Crack Depth, Varying Position of Reinforcement

If $M < M_P$, it is $P < P_P$ and, from (13) and (16), in nondimensional form it follows:

$$\frac{K_I h^{1/2} b}{P} = Y_M(\xi)\frac{M}{Ph} - Y_P\left(\frac{c}{h}, \xi\right)\frac{1}{r''\left(\frac{c}{h}, \xi\right)}\frac{M}{Ph} \quad \ldots\ldots\ldots\ldots\ldots\ldots (17)$$

while, when $M > M_P$, we have $P = P_P$ and (16) becomes

$$\frac{K_I h^{1/2} b}{P_P} = Y_M(\xi)\frac{M}{P_P h} - Y_P\left(\frac{c}{h}, \xi\right) \quad \ldots\ldots\ldots\ldots\ldots\ldots\ldots\ldots (18)$$

If the reinforcement is yielded, we use (18), otherwise (17) must be applied when stress σ_s is lower than f_y. The first case occurs when $M/P_P h \geq r''(c/h, \xi)$ [see (15)].

In Figs. 4 and 5, the stress intensity factor K_I is reported for $c/h = 1/20$ and $c/h = 1/10$, respectively, against the crack depth ξ and varying the loading parameter $M/P_P h$. Each diagram is divided into two regions, characterized by different conditions of deformation for reinforcement. The loading conditions and crack depths for which the assumed model predicts nonyielded reinforcement are lying to the left of the separation line.

All the curves $M/P_P h$ = constant belong, partially or totally, to the domain where the reinforcement is in the elastic condition. No yielding of reinforcement is shown for $M/P_P h \lesssim 0.8$, when $c/h = 0.05$, or $M/P_P h \lesssim 0.7$, when $c/h = 0.10$ (Figs. 4 and 5).

The ascending part of the curves corresponds to an unstable crack propagation process. In Fig. 4, it appears that, beyond the value $M/P_P h \approx 1.0$, the curves are always increasing and the crack propagation (which occurs when factor K_I reaches its critical value K_{IC}) is always unstable.

Crack Propagation

Assuming that K_I is equal to the matrix fracture toughness K_{IC} from (16), we have

$$\frac{M_F}{K_{IC} h^{3/2} b} = \frac{1}{Y_M(\xi)} + \frac{P}{K_{IC} h^{1/2} b}\frac{Y_P\left(\frac{c}{h}, \xi\right)}{Y_M(\xi)} \quad \ldots\ldots\ldots\ldots\ldots\ldots\ldots (19)$$

If the force P transmitted by the reinforcement is equal to $P_P = f_y A_s$ or, in other words, if the reinforcement yielding limit has been reached ($M = M_F \geq M_P$), (19) becomes

$$\frac{M_F}{K_{IC} h^{3/2} b} = \frac{1}{Y_M(\xi)} + N_P\frac{Y_P\left(\frac{c}{h}, \xi\right)}{Y_M(\xi)} \quad \ldots\ldots\ldots\ldots\ldots\ldots\ldots (20)$$

where the brittleness number

$$N_P = \frac{f_y h^{1/2}}{K_{IC}}\frac{A_s}{A} \quad \ldots\ldots\ldots\ldots\ldots\ldots\ldots\ldots\ldots\ldots\ldots\ldots (21)$$

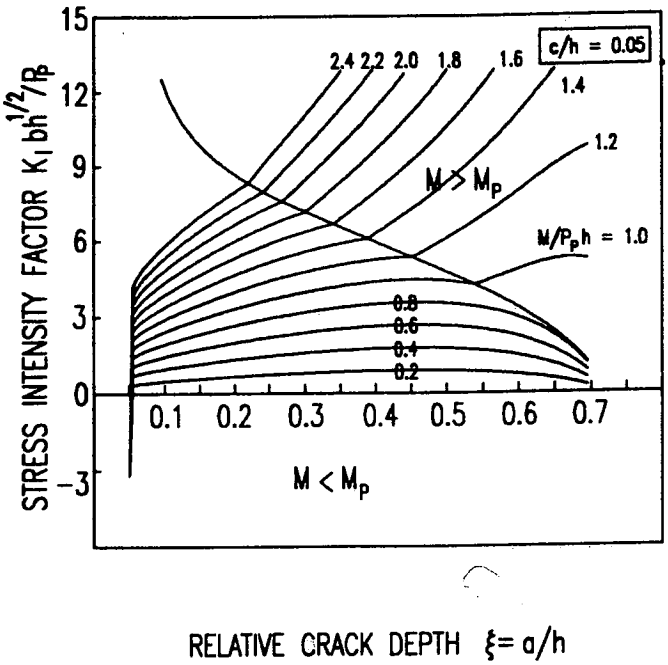

FIG. 4. Dimensionless Stress Intensity Factor versus Relative Crack Depth ξ, Varying Applied Bending Moment (c/h = 0.05)

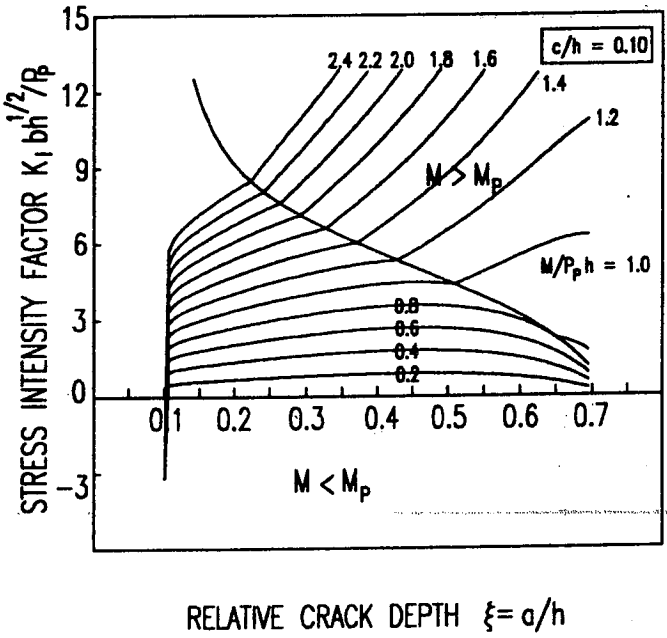

FIG. 5. Dimensionless Stress Intensity Factor versus Relative Crack Depth ξ Varying Applied Bending Moment (c/h = 0.10)

is introduced, and $A = bh$ = the total cross-section area.

In the case $M = M_F < M_P$, i.e., when the reinforcement is in the elastic condition, we can consider the relation

$$\frac{M_F}{K_{IC}h^{3/2}b} = \frac{1}{Y_M(\xi)} + N_P \frac{M_F}{M_P} \frac{Y_P\left(\frac{c}{h}, \xi\right)}{Y_M(\xi)} \quad \ldots\ldots\ldots\ldots\ldots\ldots\ldots\ldots\ldots\ldots (22)$$

since, in that case, it is $\sigma_s/f_y = M_F/M_P$, and, therefore, $P = \sigma_s A_s = f_y(M_F/M_P)A_s$ in (19).

Eq. (22) may be modified considering (15) and (21)

$$\frac{M_F}{K_{IC}h^{3/2}b} = \frac{1}{Y_M(\xi) - \dfrac{Y_P\left(\dfrac{c}{h}, \xi\right)}{r''\left(\dfrac{c}{h}, \xi\right)}} \quad \ldots\ldots\ldots\ldots\ldots\ldots\ldots\ldots\ldots\ldots\ldots\ldots (23)$$

Therefore, according to the model when $M_F < M_P$, the moment of crack propagation M_F depends only on the relative crack depth ξ and is not affected by the brittleness number N_P. It does not depend on the content of reinforcement, but only on its relative position c/h.

The dimensionless fracture moment versus crack depth ξ, is reported in Fig. 6 for $c/h = 0.05$ and by varying N_P. The curves $N_P \lesssim 0.2$ are descending over the whole range ξ. This means that for low reinforced beams and/or for large cross sections, the fracture bending moment decreases while the crack extends. An unstable fracture phenomenon occurs.

For higher N_P values, the model predicts a stable fracture process with deep cracks. In particular, this occurs for $N_P \geqslant 0.3$.

Moment versus Rotation Response

The local rotation due to the applied loads is given by a superimposed effect in the following way:

$$\Delta\varphi = \lambda_{MM}M - \lambda_{MP}P \quad \ldots\ldots\ldots\ldots\ldots\ldots\ldots\ldots\ldots\ldots\ldots\ldots\ldots\ldots (24)$$

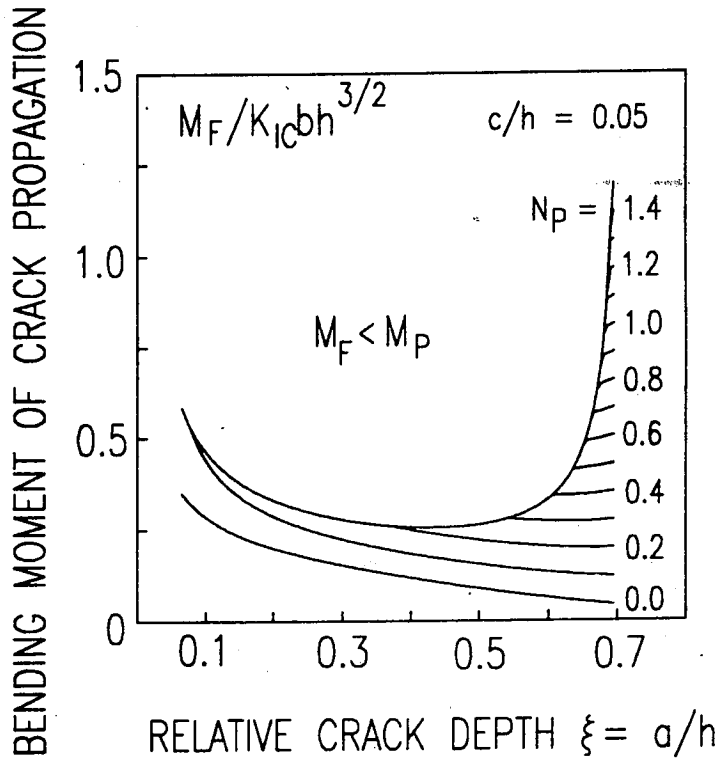

FIG. 6. Dimensionless Bending Moment of Crack Propagation versus Relative Crack Depth ξ, Varying Brittleness Number N_P ($c/h = 0.05$)

where λ_{MP} is obtained from (10) and λ_{MM} from (Carpinteri 1984)

$$\lambda_{MM} = \frac{2}{bh^2E}\int_0^{\xi} Y_M^2(\xi)\, d\xi \quad \ldots\ldots (25)$$

For the relative crack depth ξ, let $\Delta\varphi_F$ be the local rotation due to the presence of a crack when the applied bending moment reaches the value M_F. However, it is possible to define the local rotation $\Delta\varphi_{F0}$ for the initial relative crack depth ξ_0 at the moment of crack propagation.

For $M = M_F$, (24) can be written as

$$\Delta\varphi_F = \lambda_{MM}M_F - \lambda_{MP}P_P\alpha \quad \ldots\ldots (26)$$

with $\alpha = M_F/M_P = P/P_P < 1$ if $M_F < M_P$; and $\alpha = 1$ if $M_F \geq M_P$.

Eq. (26) can be expressed as a function of the relevant geometrical parameters of the cracked element. To this purpose, assuming $K_I = K_{IC}$ in (16), it is

$$K_{IC} = \frac{M_F}{h^{3/2}b}\, Y_M(\xi) - \frac{P}{h^{1/2}\, b}\, Y_P\left(\frac{c}{h}, \xi\right) \quad \ldots\ldots (27)$$

and considering that $P = P_P\alpha$, it follows

$$M_F = \frac{K_{IC}h^{3/2}b}{Y_M(\xi)} + \frac{Y_P\left(\frac{c}{h}, \xi\right)}{Y_M(\xi)} P_P h\alpha \quad \ldots\ldots (28)$$

Taking into account (28), (26) is rewritten as

$$\Delta\varphi_F = \lambda_{MM}\left[\frac{K_{IC}h^{3/2}b}{Y_M(\xi)} + \frac{Y_P\left(\frac{c}{h}, \xi\right)}{Y_M(\xi)} P_P h\alpha\right] - \lambda_{MP}P_P\alpha \quad \ldots\ldots (29)$$

which, with the position

$$r'\left(\frac{c}{h}, \xi\right) = \frac{\int_{c/h}^{\xi} Y_M(\xi)Y_P\left(\frac{c}{h}, \xi\right) d\xi}{\int_0^{\xi} Y_M^2(\xi)\, d\xi} = \frac{\lambda_{MP}}{\lambda_{MM}h} \quad \ldots\ldots (30)$$

and considering (21), becomes

$$\Delta\varphi_F = \lambda_{MM}\frac{K_{IC}bh^{3/2}}{Y_M(\xi)}\left\{1 + \left[Y_P\left(\frac{c}{h}, \xi\right) - r'\left(\frac{c}{h}, \xi\right) Y_M(\xi)\right]N_P\alpha\right\} \quad \ldots (31)$$

In (31), we should always consider that $\alpha < 1$ if $M_F < M_P$ or $\alpha = 1$ if $M_F \geq M_P$. In fact, we cannot explicitly obtain M_F or M_P. However, to obtain the coefficient α, only the knowledge of their ratio is needed. To this purpose, from (28) and (15), we obtain

$$\alpha = \frac{M_F}{M_P} = \frac{K_{IC} b h^{3/2}}{P_P h Y_M(\xi) r''\left(\frac{c}{h}, \xi\right)} + \frac{Y_P\left(\frac{c}{h}, \xi\right)}{Y_M(\xi) r''\left(\frac{c}{h}, \xi\right)} \frac{M_F}{M_P} \quad \ldots\ldots\ldots\ldots (32)$$

Then, considering (21), it follows:

$$\frac{M_F}{M_P}\left[1 - \frac{1}{r''\left(\frac{c}{h}, \xi\right)} \frac{Y_P\left(\frac{c}{h}, \xi\right)}{Y_M(\xi)}\right] = \frac{1}{N_P r''\left(\frac{c}{h}, \xi\right) Y_M(\xi)} \quad \ldots\ldots\ldots\ldots (33)$$

and finally

$$\alpha = \frac{M_F}{M_P} = \frac{1}{\left[Y_M(\xi) r''\left(\frac{c}{h}, \xi\right) - Y_P\left(\frac{c}{h}, \xi\right)\right] N_P}, \quad \text{for} \quad M_F < M_P \ldots (34)$$

while $\alpha = 1$ when $M_F \geq M_P$.

From (31) and (34), it should then be possible to obtain the normalized rotation $\Delta\varphi_F/K_{IC} b h^{3/2}$ varying the brittleness number N_P for a given relative crack depth ξ. However, it is possible to consider the ratio $\Delta\varphi_F/\Delta\varphi_{F0}$ between the values given by (31) for $\xi > \xi_0$ and $\xi = \xi_0$, respectively, and to plot a diagram where $M_F/K_{IC} b h^{3/2}$, given by (20) or (23), is considered the vertical axis. In this case, in fact, if crack propagation is seen as an evolutive phenomenon, ξ giving the subsequent positions of the crack tip, the normalized bending moment-versus-rotation diagram is obtained until the cracking phenomenon develops up to the complete disconnection of the cross section.

Then, for defined geometry and toughness characteristics, the constitutive behavior of a cracked section is well-described by the brittleness number N_P.

In Figs. 7(*a*)–7(*e*), the moment-rotation diagrams are reported for N_P = 0 (no reinforcement), 0.1, 0.26, 0.53, and 0.87, corresponding to the values planned for an experimental campaign on reinforced concrete beams (Bosco et al. 1990a). The same figures also show the ultimate carrying capacity and the asymptotical behavior (dotted horizontal lines) when the cross section is completely cracked and the reinforcement is yielded. Since the resultant tensile force is located at $(h - c)$ from the upper edge of the cross section, the ultimate bending moment results to be $M_u = P_P(h - c)$.

Considering that $N_P = P_P h/(K_{IC} b h^{3/2})$, it is possible to obtain $M_u/(K_{IC} b h^{3/2}) = N_P(h - c)/h$, that is, the limit value to which the normalized moment-rotation curves tend, for every defined value of N_P. It is worth noting that for sufficiently high concrete strength and sufficiently low percentage of steel, this type of failure precedes crushing of the matrix.

Figs. 7(*a*)–7(*e*) illustrate the failure mechanisms given by the model, varying the brittleness number N_P. The following remarks can be made.

1. In Figs. 7(*b*) and 7(*c*) (where N_P = 0.1 and 0.26 both represent a very low percentage of reinforcement or a deep cross section), the contributions of the reinforcement do not involve any appreciable increase in the load-bearing

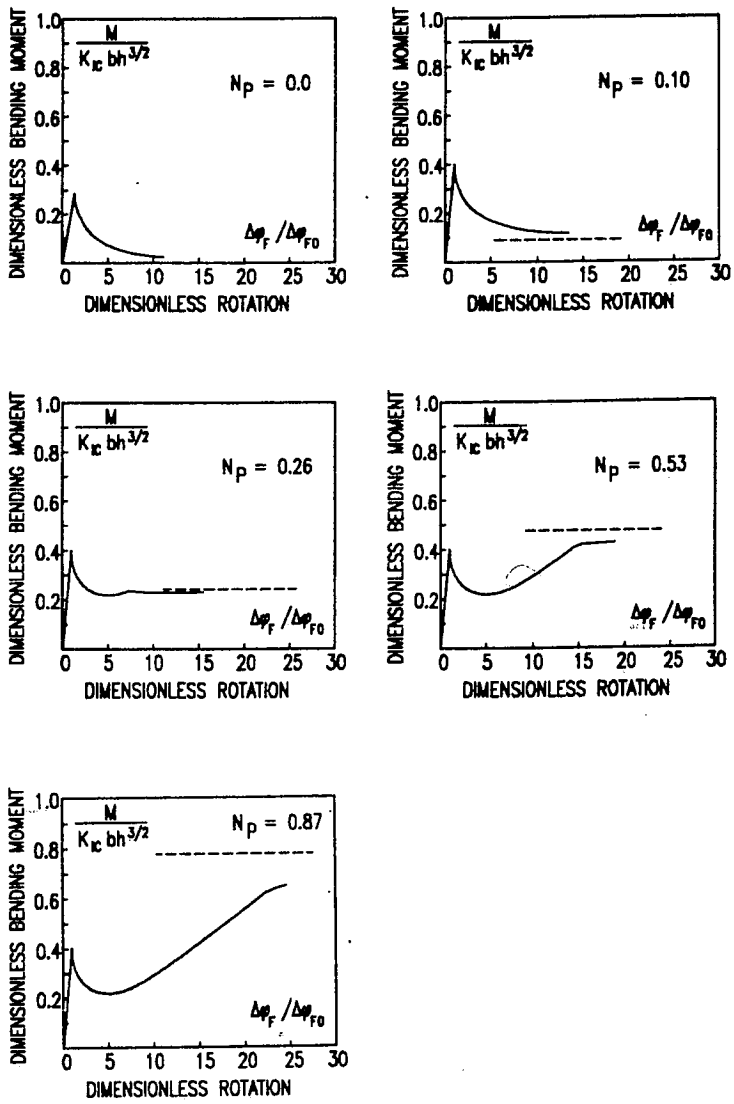

FIG. 7. Normalized Moment-Rotation Curves, Varying Brittleness Number N_P

capacity with regard to the plain cross section. Then the phenomenon of crack propagation is markedly unstable. The first cuspidal point represents the first cracking, whereas, the second represents steel yielding.

2. In Figs. 7(*d*) and (*e*) (where $N_P = 0.53$ and 0.87), the benefit of the reinforcement is manifested, and the resistant bending moment increases, becoming greater than M_F. The phenomenon changes from unstable to stable, and the failure mode does not result in brittleness if it is strain-controlled. However, a snap-through instability is predicted if the process is load-controlled.

Comparison with Experimental Results

The experimental behavior of concrete elements with a low steel percentage is influenced by a number of aspects that are usually neglected, yet play a significant role. Namely, the experimental results are influenced by nonlinear effects. In particular, the value M_F is affected by the nonlinearity of tensile stress-strain relationship of concrete at the onset of first cracking, while the bending moment M_P is influenced by the stress-versus-crack opening displacements relationship.

However, though the influence of the aforementioned nonlinearities exists, the experimental results on a series of 30 high-strength concrete beams (Bosco et al. 1990b) revealed that keeping the scale constant and varying

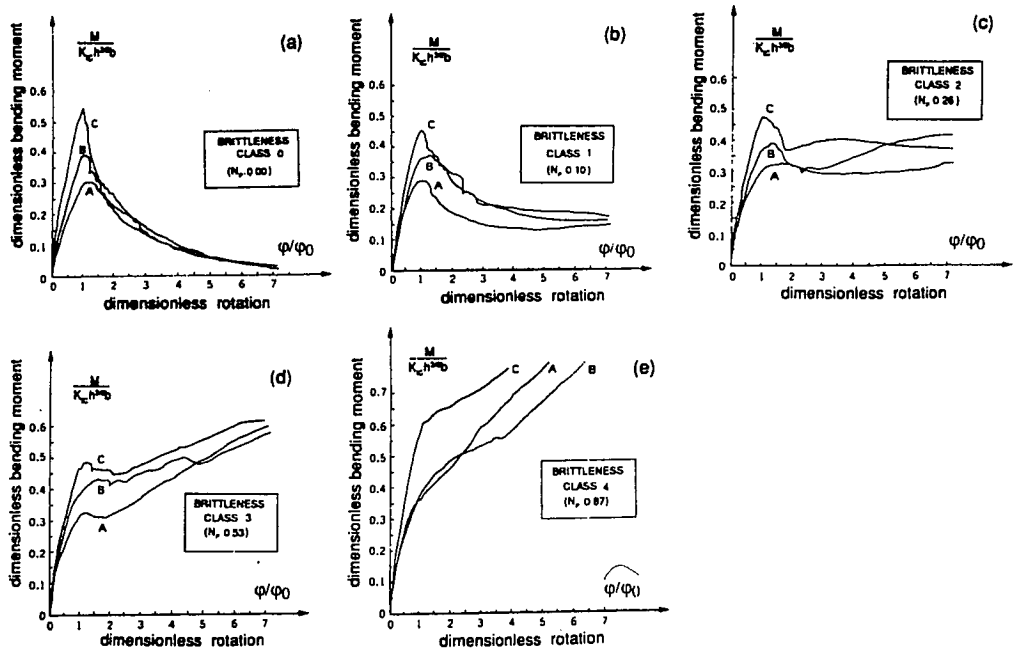

FIG. 8. Experimental Moment-Rotation Curves, for High-Strength Concrete Beams, Varying Brittleness Number N_P

the steel content, the phenomenon of crack propagation changes from stable to unstable, and the transition occurs at an order of magnitude of N_P as that predicted by LEFM.

The dimensionless bending moment-versus-rotation curves obtained from the tests are grouped in brittleness classes in Figs. 8(*a*) to 8(*e*), the brittleness number varying from zero to 0.87.

The local rotation is normalized with respect to the value $\Delta\varphi_{F0}$ recorded at the first cracking and is related to the central beam element of length equal to the beam depth h. The bending moment, however, is nondimensionalized with respect to the critical value of the stress intensity factor of concrete, K_{IC}, and the beam depth h.

The diagrams are significant only for $\Delta\varphi_F/\Delta\varphi_{F0} > 1$, the strain softening and curvature localization occurring only after the first cracking. The dimensionless peak moment does not appear to be the same when the brittleness class is the same and the beam depth is varied. This occurs because reference is made to typical fracture mechanics parameters, whereas, the cross section is initially unnotched. However, the postpeak branches are very close to each other and present the same shape for each selected brittleness class. The size-scale similarity seems, then, to govern the postpeak behavior, especially for low brittleness numbers N_P.

The same brittleness transition theoretically predicted in Fig. 7, is reproposed by the experimental diagrams in Fig. 8 approximately for $N_P = N_{PC} = 0.26$.

CONCLUSIONS

1. From the results obtained, it appears clear that even by using different congruence conditions (Carpinteri 1984), the compliance model always allows the description of ductile as well as brittle failure behavior in structural elements with low content of reinforcement or deep cross section. The brittleness number N_P is the parameter able to represent the transition between the two failure modes.

2. Important results arise when the global response is investigated. By using the crack opening displacement congruence condition, a global response in terms of the moment-rotation curve is obtained, which is very similar to the experimental one, at least when low reinforced concrete beams are considered.

3. This theoretical model seems to represent the actual behavior of reinforced concrete elements satisfactorily, both with low content of reinforcement and deep cross section. Softening and snap-through instabilities are revealed by the model as well as they are observed experimentally.

4. Although LEFM represents a simplification of reality, the model provides useful information and, substantially, consistent prediction, especially for high-strength concrete, which is a very brittle material.

5. If a minimum reinforcement amount is related to the condition when the first peak moment is equal to the plastic limit moment, its theoretical value results of the same order of magnitude as that required by the most important standard codes. However, the minimum reinforcement, according to the model, decreases with the beam depth (Bosco et al. 1990b).

Acknowledgments

The writers gratefully acknowledge the financial support of the National Research Council (CNR) and the Department for University and Scientific and Technological Research (MURST).

Appendix I. References

Bosco, C., Carpinteri, A., and Debernardi, P. G. (1990a). "Fracture of reinforced concrete: Scale effect and snap-back instability." *Engrg. Fract. Mech.*, 35(4–5), 665–677.

Bosco, C., Carpinteri, A., and Debernardi, P. G. (1990b). "Minimum reinforcement in high-strength concrete." *J. Struct. Engrg.*, ASCE, 116(2), 427–437.

Carpinteri, A. (1981). "A fracture mechanics model for reinforced concrete collapse." *IABSE Colloquium on Advanced Mech. of Reinforced Concr.*, Delft, 17–30.

Carpinteri, A. (1984). "Stability of fracturing process in RC beams." *J. Struct. Engrg.*, ASCE, 110, 544–558.

Okamura, H., Watanabe, K., and Takano, T. (1973). "Applications of the compliance concepts in fracture mechanics." *ASTM STP 536*, American Society for Testing and Mater. (ASTM), Philadelphia, Pa., 423–438.

Okamura, H., Watanabe, K., and Takano, T. (1975). "Deformation and strength of cracked member under bending moment and axial force." *Engrg. Fract. Mech.*, 7, 531–539.

Tada, H., Paris, P., and Irwin, G. (1963). *The stress analysis of cracks handbook.* Vol. 2, Del Research Corp., St. Louis, Mo., 16–17.

Appendix II. Notation

The following symbols are used in this paper:

A = cross-sectional area of beam;
A_s = total cross-sectional area of reinforcement;
a = crack length;
b = total width of cross section;
c = vertical distance between reinforcement and lower edge of beam;
E = Young's modulus for concrete;

f_y = yield strength of reinforcement;
h = total depth of cross section;
K_I = stress-intensity factor;
K_{IC} = critical value of stress-intensity factor;
K_{IM} = stress-intensity factor provoked by bending moment;
K_{IP} = stress-intensity factor provoked by applied forces;
M = applied bending moment;
M_F = bending moment of crack propagation;
M_P = bending moment of reinforcement plastic flow;
M_u = ultimate resistant bending moment;
N_P = brittleness number, (21);
P = applied force (on crack surface);
P_P = yielding force of reinforcement;
α = M_F/M_P;
$\Delta\delta$ = total crack opening displacement (at points where forces P are applied);
$\Delta\delta_{PM}$ = crack opening displacement (at points where forces P are applied) due to bending moment;
$\Delta\delta_{PP}$ = crack opening displacement (at points where forces P are applied) due to applied forces P;
$\Delta\varphi$ = local rotation at cracked cross section;
$\Delta\varphi_F$ = local rotation at cracked cross section when crack propagation occurs for relative crack depth ξ;
$\Delta\varphi_{F0}$ = local rotation at cracked cross section when first crack propagation occurs (relative crack depth ξ_0);
$\Delta\varphi_{MP}$ = local rotation of cracked cross section due to applied forces P;
λ_{MM} = rotational compliance due to bending moment;
λ_{MP} = rotational compliance due to applied forces;
λ_{PM} = opening compliance due to bending moment;
λ_{PP} = opening compliance due to applied forces;
ξ = relative crack depth a/h;
ξ_0 = initial relative crack depth a_0/h; and
σ_s = stress in reinforcement.